Aerodynamic Modeling of ATTAS Aircraft Using Mamdani Fuzzy Inference Network

ARUN K. SHARMA, Student Member, IEEE
DHANJEET SINGH, Student Member, IEEE
VIKAS SINGH, Student Member, IEEE
NISHCHAL K. VERMA, Senior Member, IEEE
Department of Electrical EngineeringIndian Institute of Technology Kanpur, Kanpur 208016, India

This article presents aerodynamic modeling of the fixed-wing aircraft using the Mamdani fuzzy inference network (MFIN). A Mamdani fuzzy inference system with a Gaussian membership function has been used as a nonlinear regression functional node to create a multilayer network, called MFIN. The multilayered MFIN incorporates the nonlinear function approximation capability of the multilayered neural network in addition to robustness against uncertainties and measurement noises. The limited-memory Broyden–Fletcher–Goldfarb–Shanno optimization technique has been used to optimize network parameters to learn the nonlinear yawing moment dynamics of the Advanced Technology Testing Aircraft System (ATTAS) aircraft. Since every node in the network learns the nonlinearity of the dynamics, the proposed MFIN becomes capable of learning highly nonlinear dynamics. The adequacy of the proposed network is validated using the recorded flight data from the ATTAS aircraft of the DLR German Aerospace Centre in two cases: 1) trimmed low-angle-of-attack flight condition and 2) quasi-steady stall high-angle-of-attack (highly nonlinear complex) flight condition. The simulated time history tracking performance, mean square error, R^2 score, and explained variance score of the proposed network are compared with state-of-the-art methods. Also, the robustness of the proposed approach is demonstrated by evaluating its performance against test data corrupted with additive white Gaussian noise.

Manuscript received February 4, 2019; revised July 20, 2019 and November 7, 2019; released for publication February 8, 2020. Date of publication February 21, 2020; date of current version October 9, 2020.

DOI. No. 10.1109/TAES.2020.2975447

Refereeing of this contribution was handled by A. Halder.

Authors' address: Arun K. Sharma, Dhanjeet Singh, Vikas Singh, and Nishchal K. Verma are with the Department of Electrical Engineering, Indian Institute of Technology Kanpur, Kanpur 208016, India E-mail: (arnksh@iit.ac.in; dhanjeet@iitk.ac.in; vikkyk@iitk.ac.in; nishchal@iitk.ac.in). *(Corresponding author: Arun K. Sharma.)*

I. INTRODUCTION

An accurate mathematical model of aircraft dynamics plays a vital role in the design and development of flight control laws, analysis and understanding of the behavior of the aircraft, capability enhancement, and system upgrade activities. Aerodynamic modeling is the mathematical modeling of the aircraft considering mainly the effect of aerodynamic forces and moments on the dynamics of the aircraft. The aerodynamic model can be determined either by an experimental (wind-tunnel) method or by a parameter estimation method. The experimental method requires an experimental setup, which is generally costly. Therefore, modeling based on the input–output data pair is gaining popularity for such systems, as reported in various literature works [1]–[4]. System parameter estimation or modeling based on input–output flight data is known as system identification methods.

In the past, various statistical methods of system identification have been widely used to identify parameters of the aircraft system [5]–[8]. In general, the output error, maximum likelihood estimation (MLE), and the filter error are the most popular statistical methods for system identification [7], [8], [10]. Recent computational intelligence (CI)-based methods, such as the artificial neural network (ANN) [11]–[14] and deep learning [15], [16], are being applied for aerodynamic modeling, parameter estimation, and fault detection. Nowadays, after the evolution of fast computational resources, deep-learning-based methods are becoming very popular due to their nonlinear function mapping capability.

Similar to aforementioned approaches, fuzzy-based CI tools, such as fuzzy logic systems and fuzzy inference systems, have gained much attention from various researchers [17]–[23]. In [20]–[23], the fuzzy inference system (FIS) has been proved to be a very effective tool for system identification in numerous engineering or nonengineering applications. The FIS is a very powerful computational tool for modeling nonlinear complex systems due to its interpretability. Fuzzy-based aerodynamic modeling and control exhibits many advantages compared to physics-based modeling or ANN-based approximation [24]–[26], for example, integrating linguistic information from human experts with numerical data and representation of highly nonlinear complex models as linear models. Therefore, various fuzzy-based computational tools have been developed and applied in numerous real-world applications, e.g., design of a room temperature and humidity controller, transportation, decision support systems, washing machine, crime investigation, condition-based monitoring etc. [20]–[23], [27], [28].

Saderla *et al.* [29] showed that the neural Gauss–Newton method, free from solving any equations of motion, performs on a par with the MLE method for the estimation of aerodynamic parameters from near stall flight data. In [30], a radial basis function network (RBFN) has been used for the estimation of lateral–directional force and moment coefficients of the ATTAS aircraft. The stability and control derivatives are estimated using the neural partial differentiation method. In [18], the yawing moment coefficient of the ATTAS aircraft is modeled using the Takagi–Sugeno (T-S) fuzzy modeling method. In [31], the estimation of the angle of attack of the ATTAS aircraft has been described using an interval type-2 (IT-2) T-S FIS, where the FIS has been treated as a system identification tool to estimate the angle of attack using sensor data of linear acceleration, air speed, and pitch angle. The application of the IT-2 T-S FIS enhances the robustness of the method against data uncertainties. In these methods, fuzzy reasoning handles uncertainties in the data, but human-expert-based knowledge of cause and effect available in linguistic form cannot be incorporated because the consequent part in the T-S FIS is a linear algebraic function. Also, the performance of the T-S fuzzy model deteriorates if the measurement noise in the test data increases.

In [32], recorded flight data have been used to generate the Mamdani FIS, where human-expert-based knowledge can also be incorporated to the fuzzy rule base (FRB) of the Mamdani FIS. This tool of system identification acts as a single node of the Mamdani-type FIS and gives commendable accuracy for the estimation of the aircraft yawing moment coefficient. Also, it may underfit for highly nonlinear complex dynamics and fail to correctly predict the output for test data. Verma *et al.* [27] have proposed a single-hidden-layer neural network (NN) for system identification of complex and nonlinear problems. This method needs large memory and high computational resources even for a simpler problem, as shown in [28], and may succumb to the out-of-memory problem if complexity of the problem or dimensionality of the input data increases.

To overcome the aforementioned limitations of the existing methodologies, this article presents the Mamdani fuzzy inference network (MFIN) with an advanced limited-memory Broyden–Fletcher–Goldfarb–Shanno (L-BFGS) optimization technique for network parameter search. The proposed approach uses the Mamdani FIS described in [32] as a nonlinear regression functional node to create a multilayer network, which is trained to learn the nonlinear dynamics of the yawing moment coefficient of the ATTAS aircraft using the recorded flight data. L-BFGS optimization is implemented with a parallel computational toolbox in MATLAB. The proposed MFIN gives: 1) improved accuracy; 2) capability to incorporate expert knowledge in linguistic form; 3) improved capability of handling data uncertainties; and 4) robustness to additive white Gaussian noise (AWGN) that may be introduced in the test data during measurement/recording.

The rest of this article is organized as follows. Section II briefs the physics of the fixed-wing aircraft lateral–directional aerodynamics to model the yawing moment coefficient on the recorded flight data. Section III describes the detailed methodology for the design and training of the proposed network. In Section IV, simulation results of the proposed network have been validated on flight data of the ATTAS aircraft and compared with other state-of-the-art methods of system identification. Finally, Section V concludes this article.

II. FIXED-WING AIRCRAFT LATERAL–DIRECTIONAL AERODYNAMICS

The lateral–directional forces and moments on the aircraft produce transnational deflection along the pitch axis and rotational motions about the roll and yaw axes. The equations of motion in the lateral direction [33], [34] are given as

$$m(\dot{v} + ru - pw) = mg\sin\phi\cos\theta + F_y \tag{1}$$

$$\dot{p}I_{xx} + qr(I_{zz} - I_{yy}) - (\dot{r} + pq)I_{xz} = \bar{L} \tag{2}$$

$$\dot{r}I_{zz} + pq(I_{yy} - I_{xx}) - qr - \dot{p})I_{xz} = \bar{N} \tag{3}$$

where m is the total mass of the aircraft; $u, v,$ and w are the linear velocity components; $p, q,$ and r are the angular velocity components along x, y, and z axes, respectively; and ϕ and θ are the roll and pitch angles, respectively. $I_{xx}, I_{yy},$ and I_{zz} are the inertia parameters along the x, y, and z axes, respectively, F_y is the total force along the y-axis, and $\bar{L}$ and $\bar{N}$ are the moments about the x and z axes, respectively. The lateral aerodynamic of an aircraft is mostly dependent on the side slip angle β, the roll rate p, the yaw rate r, the deflection of the rudder δ_r, and the deflection of the aileron δ_a. The external forces and moments [35] can be represented as follows:

$$F_y = \frac{1}{2}\rho V^2 S \times C_Y(\beta, p, r, \delta_r) \times \beta \tag{4}$$

$$\bar{L} = \frac{1}{2}\rho V^2 Sb \times C_l(\beta, p, r, \delta_a) \tag{5}$$

$$\bar{N} = \frac{1}{2}\rho V^2 Sb \times C_n(\beta, p, r, \delta_r) \tag{6}$$

where S denotes the wing surface area, ρ is the air density, b is the wing span, and V is the resultant aircraft speed. C_Y, C_l, and C_n are the nondimensional aerodynamic coefficients, which are highly nonlinear in their constitutive parameters β, p, r, δ_a, and δ_r. In the fixed-wing aircraft, stall is the most important unsteady flow phenomenon, which is observed if the angle of attack reaches a value where the flow separates from the wing and causes a drastic loss of lift. Under stall conditions, dangerously optimistic estimates of aerodynamic forces and moments are experienced by the aircraft. At low or moderate angles of attack, the airflow over the wing is laminar and stays attached to the wing to produce the desired lift. When the angle of attack exceeds the critical stall angle, the airflow begins to separate, which causes an abrupt drop in the lift produced by the wing, which can lead to turbulent behavior and catastrophic results for the aircraft. Hence, high-angle-of-attack maneuvering flight conditions (poststall maneuvering) can be categorized as complex and highly nonlinear phenomena. In these flight conditions, the aerodynamic model of forces and moments becomes a nonlinear function of β, p, r, δ_a, and δ_r [35].

For small variation of state and control input parameters, the side force, rolling, and yawing moment coefficients [35]

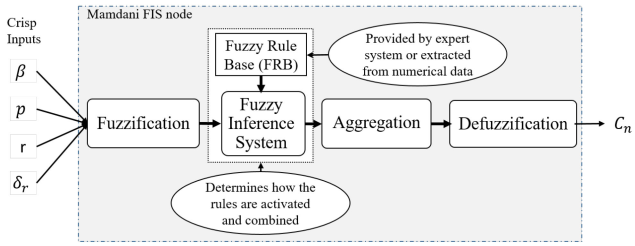

Fig. 1. Mamdani FIS node.

can be modeled with acceptable accuracy using linear approximations as

$$C_Y(\beta, p, r, \delta_r) = C_{Y_0} + C_{Y_\beta}\beta + C_{Y_p}\frac{pb}{2V} + C_{Y_r}\frac{rb}{2V} + C_{Y_{\delta_r}}\delta_r \tag{7}$$

$$C_l(\beta, p, r, \delta_a) = C_{l_0} + C_{l_\beta}\beta + C_{l_p}\frac{pb}{2V} + C_{l_r}\frac{rb}{2V} + C_{l_{\delta_a}}\delta_a \tag{8}$$

$$C_n(\beta, p, r, \delta_r) = C_{n_0} + C_{n_\beta}\beta + C_{n_p}\frac{pb}{2V} + C_{n_r}\frac{rb}{2V} + C_{n_{\delta_r}}\delta_r \tag{9}$$

where the coefficients $C_{n_0}, C_{n_\beta}, C_{n_p}, C_{n_r}, C_{n_{\delta_r}}$, $C_{Y_0}, C_{Y_\beta}, C_{Y_p}, C_{Y_r}, C_{Y_{\delta_r}}$, $C_{l_0} C_{l_\beta}, C_{l_p}, C_{l_r}$, and $C_{l_{\delta_a}}$ are the stability and control derivatives pertaining to lateral–directional motion of the aircraft.

Suitable formulation of the aerodynamic model can be characterized as phenomenological models and behavioral models. Phenomenological models are derived based on basic principles and the physical law describing the process, while behavioral models can be generated from input and output data without any specific relevance to the internal behavior of the process. In this article, behavioral models of the yawing moment aerodynamic coefficient (C_n) are derived by the MFIN on the recorded flight data.

III. MAMDANI FUZZY INFERENCE NETWORK

System identification using the FIS has been widely reported in various literature works [36]–[39]. In [32], the recorded flight data were used to generate the Mamdani FIS for the estimation of the yawing moment coefficient of the ATTAS aircraft. In the proposed approach, the Mamdani FIS used for system identification in [32] is treated as a nonlinear regression functional node. Such nodes are interconnected to create a neural network, which can approximate a highly nonlinear complex function along with fuzziness in the input–output data. The network created using such nodes is term as the MFIN. The MFIN may consist of an input layer, multiple hidden layers, and an output layer, as shown in Fig. 5. The output layer may consist of a Mamdani FIS node or a linear regression node. The process of input–output mapping through each node is depicted in Fig. 1, and details can be found in [32].

The FIS node in the network consists of the FRB. The FRB of a Mamdani node has several "IF–THEN" rules with fuzzy proposition in both premise and consequence parts. The parameters associated with each FIS node in the network may be different. The operators used in the fuzzy inference process determine the mathematical model of each node. The nonlinear regression functional node is, in general, nondifferentiable; therefore, advanced optimization techniques have been used for identifying the parameters of the MFIN.

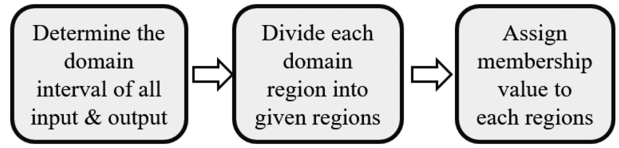

Fig. 2. Procedure to create fuzzy regions.

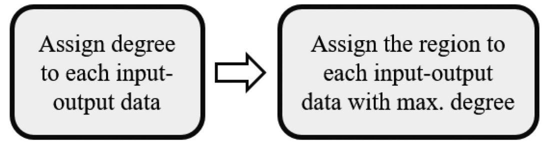

Fig. 3. Find MF degree for a data point.

A. Fuzzy Rule Base

The FRB is a collection of linguistic "IF–THEN" rules, which defines how the FIS node makes decisions with respect to the given inputs. For examples, if β, p, r, and δ_r are the inputs and C_n is the output, then the FRB with i rule is expressed as

$$\begin{aligned} R^1 :\ & \text{IF } \beta^1 \text{ is } \psi_1^1 \text{ AND } p^1 \text{ is } \psi_2^1 \text{ AND } r^1 \text{ is } \psi_3^1 \\ & \text{AND } \delta_r^1 \text{ is } \psi_4^1 \ \text{ THEN } C_n^1 \text{ is } \psi_5^1 \\ R^2 :\ & \text{IF } \beta^2 \text{ is } \psi_1^2 \text{ AND } p^2 \text{ is } \psi_2^2 \text{ AND } r^2 \text{ is } \psi_3^2 \\ & \text{AND } \delta_r^2 \text{ is } \psi_4^2 \ \text{ THEN } C_n^2 \text{ is } \psi_5^2 \\ & \qquad \vdots \\ R^i :\ & \text{IF } \beta^i \text{ is } \psi_1^i \text{ AND } p^i \text{ is } \psi_2^i \text{ AND } r^i \text{ is } \psi_3^i \\ & \text{AND } \delta_r^i \text{ is } \psi_4^i \ \text{ THEN } C_n^i \text{ is } \psi_5^i \end{aligned}$$

where ψ_1^i, ψ_2^i, ψ_3^i, and ψ_4^i are various fuzzy regions in the given universe of discourse. Input membership function (IPMF) parameters govern the shape of input fuzzy membership functions (MFs) (i.e., input linguistic information), whereas output membership function (OPMF) parameters govern the shape of output fuzzy MFs (i.e., output linguistic information). The IPMF of input features (premise part: IF ...) and the OPMF of output features (consequent part: ...THEN) may be different. If the Gaussian MF is considered as the IPMF and the OPMF, then mean and standard deviation of each fuzzy region at every nodes are learnable parameters.

The detailed steps of generating an FRB of the Mamdani FIS Node and thereby creating an FIS node can be found in [32] and is briefly presented as follows:

1) create fuzzy subsets (regions) by dividing data spaces into fuzzy subsets (regions) and allocate a suitable fuzzy MF to each subset as shown in Fig. 3;

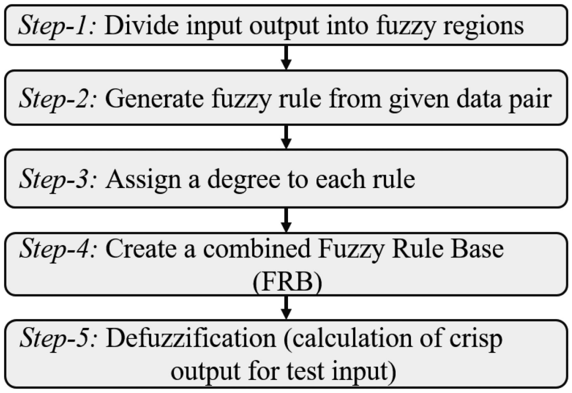

Fig. 4. Algorithmic steps to create the Mamdani FIS node.

2) find the MF grade for each feature of a data sample in the fuzzy regions created in the previous step as shown in Fig. 4;
3) use T-norm to assign an MF value to each rule based on either (10) or (11):

$$\mathrm{Deg}(R^i) = \mu_{\psi_1^i}(\beta) \wedge \mu_{\psi_2^i}(p) \wedge \mu_{\psi_3^i}(r) \wedge \mu_{\psi_4^i}(\delta_r) \wedge \mu_{\psi_5^i}(C_n) \quad (10)$$

$$\mathrm{Deg}(R^i) = \mu_{\psi_1^i}(\beta) * \mu_{\psi_2^i}(p) * \mu_{\psi_3^i}(r) * \mu_{\psi_4^i}(\delta_r) * \mu_{\psi_5^i}(C_n) \quad (11)$$

where $\mathrm{Deg}(R^i)$ denotes the MF grade of the ith rule and $\wedge$ the "min" operation;
4) now, combine the rules generated from numerical data and the expert opinions (linguistic rules) and then remove the conflict to get the final FRB. If multiple rules consist of the common premise, but different consequences, the rule with the largest value of the MF grade is considered;
5) if N is the total number of rules in the FRB, the estimated output $\hat{C}_n$ of the FIS node is calculated by defuzzification of the aggregated fuzzy output. Here, we use the center of gravity for defuzzification, as follows:

$$\hat{C}_n = \frac{\sum_{i=1}^{N} \overline{C}_n^i \mu_i^o}{\sum_{i=1}^{N} \mu_i^o} \quad (12)$$

where $\overline{C}_n^i$ is the center of mass and μ_i^o is the MF grade of the ith rule in the output fuzzy subset for a given test input and is calculated as

$$\mu_i^o = \mu_{\psi_1^i}(\beta) \wedge \mu_{\psi_2^i}(p) \wedge \mu_{\psi_3^i}(r) \wedge \mu_{\psi_4^i}(\delta_r). \quad (13)$$

The algorithmic steps to create the Mamdani FIS node is summarized in Fig. 4.

B. Proposed Architecture

The proposed MFIN is a multilayered neural network (ML-NN) created by Mamdani FIS nodes, as shown in Fig. 5. The weight connecting the nodes in different layers is considered as unity. The output of each node is calculated based on the Mamdani FIS, as described in Section III-A.

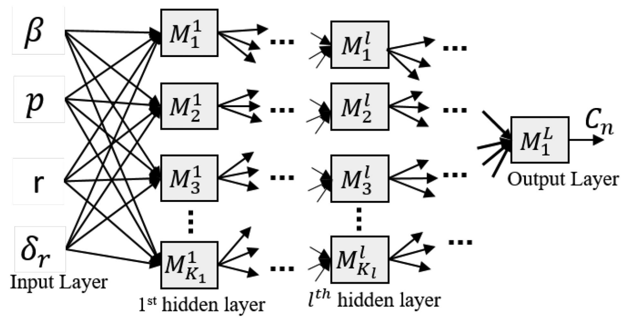

Fig. 5. Mamdani fuzzy inference network.

The output of each hidden layer is considered as the input for each node in the next layer. The network architecture, that is, the number of hidden layers and the IPMF for each node in a layer, can be chosen based upon the complexity and nonlinearity of the problem. The size of input and output layers is decided by the number of input and output features, respectively.

If L is the total number of layers, K_l is the number of nodes in the lth layer, and ν_l is the number of fuzzy regions for the FIS node in the lth layer, then the input parameter matrix $\Omega^{i,l,k}$ and the output parameter matrix $\Omega^{O,l,k}$ for the lth layer and the kth node can be, respectively, written as

$$\Omega^{i,l,k} = \begin{bmatrix} \mu_{1,1}^{i,l,k} & \sigma_{1,1}^{i,l,k} & \cdots & \mu_{1,\nu_l}^{i,l,k} & \sigma_{1,\nu_l}^{i,l,k} \\ \vdots & \vdots & \ddots & \vdots & \vdots \\ \mu_{j,1}^{i,l,k} & \sigma_{j,1}^{i,l,k} & \cdots & \mu_{j,\nu_l}^{i,l,k} & \sigma_{j,\nu_l}^{i,l,k} \\ \vdots & \vdots & \ddots & \vdots & \vdots \\ \mu_{K_{l-1},1}^{i,l,k} & \sigma_{K_{l-1},1}^{i,l,k} & \cdots & \mu_{K_{l-1},\nu_l}^{i,l,k} & \sigma_{K_{l-1},\nu_l}^{i,l,k} \end{bmatrix} \quad (14)$$

$$\Omega^{O,l,k} = \begin{bmatrix} \mu_{1,1}^{O,l,k} & \sigma_{1,1}^{O,l,k} & \cdots & \mu_{1,\nu_l}^{O,l,k} & \sigma_{1,\nu_l}^{O,l,k} \end{bmatrix} \quad (15)$$

where $j = 1, 2, \ldots, K_{l-1}$; K_{l-1} denotes the number of nodes in the $(l-1)$th layer, i.e., number of inputs for the lth layer.

C. Training the MFIN

The MFIN is a function approximation tool capable of mimicking an unknown system when all the learnable parameters associated with each node are tuned to map input–output data pairs. A cost function in terms of the estimated output and the target output is defined to evaluate the function approximation capability of the MFIN, as follows:

$$J = \frac{1}{2N} \sum_{i=1}^{N} \|\mathbf{C}_n^{(i)} - \hat{\mathbf{C}}_n^{(i)}\|^2 \quad (16)$$

where N is the total number of data samples, $\hat{\mathbf{C}}_n$ is the predicted output, and $\mathbf{C}_n$ is the target output. $\hat{\mathbf{C}}_n$ is dependent on premise (Ω^i) and consequent (Ω^O) parameters of each node in the network given by (14) and (15). Therefore, MFIN parameters can be obtained by solving the following equation:

$$\min_{\Omega^i,\Omega^O} J = \min_{\Omega^i,\Omega^O} \frac{1}{2N}\sum_{i=1}^{N} \|\mathbf{C}_n^{(i)} - \hat{\mathbf{C}}_n^{(i)}\|^2. \tag{17}$$

The cost function optimization objective stated in (17) is achieved by the L-BFGS [40]–[43] algorithm. The implementation of L-BFGS for the MFIN is briefly described in Section III-C1.

1) *Optimization of the MFIN Using the L-BFGS Method:* The L-BFGS algorithm is a quasi-Newton optimization technique given by the authors of [40]–[43]. It uses the hill-climbing search optimization approach to obtain a stationary point of a function. For the implementation of L-BFGS to optimize the cost function J given in (16) and (17), let us consider that the cost function J_k at current iteration is the function of the current iterate χ_k. Let us define the quadratic convex model m_k of the objective function J_k for the current iterate χ_k as

$$m_k(\omega) = J_k + \nabla J_k^T \omega + \frac{1}{2}\omega^T B_k \omega \tag{18}$$

where B_k is the symmetric positive-definite matrix known as the Hessian approximation matrix and ω_k is the minimizer parameter of a convex quadratic model m_k. It is used as the search direction and defined explicitly in terms of the Hessian approximation B_k as

$$\omega_k = -B_k^{-1}\nabla J_k. \tag{19}$$

Therefore, a new value of the iterate is

$$\chi_{k+1} = \chi_k + \alpha_k \omega_k \tag{20}$$

where α_k is the step size chosen according to the Wolfe conditions given by

$$J(\chi_k + \alpha_k\omega_k) \le J(\chi_k) + c_1\alpha_k \nabla J_k^T \omega_k \tag{21}$$

$$\nabla J(\chi_k + \alpha_k\omega_k)^T \omega_k \ge c_2 \nabla J_k^T \omega_k \tag{22}$$

where $0 < c_1 < c_2 < 1$. The minimizer parameter ω_k works as search direction and is calculated using inverse Hessian approximation matrix $H_k = B_k^{-1}$ [44]. The inverse Hessian approximation matrix H_k is calculated iteratively by

$$H_{k+1} = (I - \rho_k s_k \xi_k^T) H_k (I - \rho_k \xi_k s_k^T) + \rho_k s_k s_k^T \tag{23}$$

where $\rho_k = \frac{1}{\xi_k^T s_k}$, $s_k = \chi_{k+1} - \chi_k$ and $\xi_k = \nabla J_{k+1} - \nabla J_k$. Therefore, the algorithmic steps for implementation of L-BFGS to minimize the objective function (16) are presented in Algorithm 1.

The algorithmic steps to train the MFIN under the optimization objective posed by (16) and (17) are described in Algorithm 2.

Algorithm 1: Algorithmic Steps to Implement L-BFGS.

1: **begin**
2: *Initialization:* Choose
  i starting point (χ_0),
  ii initial value of inverse Hessian approximation (H_0)
  iii convergence tolerance $= \epsilon > 0$
3: Set $k \leftarrow 0$;
4: **while** $\nabla J > \epsilon$; **do**
  i compute J_k and ∇J_k;
  ii compute minimizer (search direction) $\omega_k = -H_k \nabla J_k$;
  iii update the search point $\chi_{k+1} = \chi_k + \alpha_k\omega_k$, where α_k is evaluated from the line search method under the constraint of the Wolfe conditions (21) and (22);
  iv compute $s_k = \chi_{k+1} - \chi_k$ and $\xi_k = \nabla J_{k+1} - \nabla J_k$;
  v compute H_{k+1} using (23);
  vi set $k \leftarrow k+1$;
5: **end**
6: **end**

Algorithm 2: Algorithmic Steps: Training the MFIN.

1: **begin**
2: *Initialization:* As suggested in [45], mean (center) of all fuzzy MFs of premise and consequent parts should be initialized approximately mean of the feature space of the dataset and *SD* (σ) in the range of [0,1].
3: *Compute output (forward computation):* Evaluate the network output by computing outputs of each node in the successive layer using (12).
4: *Evaluate the cost function J*
5: *Evaluate the gradients:* Compute numerical gradient of j with respect to all the parameters. Since the mapping by each node is not differential, we use the finite-difference method [40] to compute numerical gradients.
6: *Update the parameters:* Update all parameters to satisfy the optimization objective given by (16) and (17) using L-BFGS Algorithm 1
7: **end**

IV. RESULTS AND DISCUSSION

The adequacy of the proposed MFIN model is validated on two types of recorded flight data of the ATTAS aircraft. The first type of recorded flight data belongs to the trimmed low-angle-of-attack flight condition, whereas the second type of data belongs to the quasi-steady stall high-angle-of-attack (highly nonlinear complex) flight condition. The recorded datasets are normalized using the max–min normalization preprocessing method using $x_n = (x - x_{\min})/(x_{\max} - x_{\min})$, where x is the data before preprocessing, x_n is the normalized data, and $x_{\min}$ and $x_{\max}$ are the minimum and maximum values of the data, respectively.

The normalized data pairs are split into five sets for training and testing by using the fivefold cross-validation

TABLE I
Network Architecture and Training Methods

Methodology	Architecture	Training Method	Training parameters/
ML-NN	$4 \times (40 \times 20 \times 4) \times 1$	Gradient Descent	$\eta = 0.9$ & $\alpha = 0.1$
RBFN-RLS	$4 \times 30 \times 1)$	RLS	NA
T-S FIS	4 Input MFs	RLS	NA
ANFIS	NA	NA	NA
Mamdani FIS	IPMFs = 6 & OPMFs = 9	FIS	NA
MFIN	$4 \times (4 \times 3 \times 2) \times 1$ IPMFs = 3 & OPMFs = 3	L-BFGS	NA

sampling technique to generalize the adequacy of the proposed network. To demonstrate the effectiveness of the proposed MFIN model, state-of-the-art system identification methods, i.e., ML-NN [11], radial basis function network with recursive least squares (RBFN-RLS) [30], [47], T-S FIS [38], Mamdani FIS [32], and adaptive neuro fuzzy inference system (ANFIS) [39], are also trained on the same training dataset, and the simulation results on the test dataset are compared. Time history plots of the predicted yawing moment coefficients ($\hat{C}_n$) and the true value of yawing moment coefficients (C_n) for the MFIN and the classical neural network (NN) have been presented to compare the tracking performance of the proposed model. Also, the robustness of the proposed algorithm is demonstrated by testing the model with the test data corrupted by AWGN with 50-dB SNR, 40-dB SNR, and 30-dB SNR. Performance of the proposed method is also evaluated by comparing the mean square error (MSE), the R^2 score, and the explained variance score (EVS) for each dataset in Sections IV-A and IV-B.

If $C_n = [C_n^i]_{i=1}^N$ and $\hat{C}_n = [\hat{C}_n^i]_{i=1}^N$ are the true output and the predicted output, respectively, and N is the total number of samples, then the coefficient of determination (R^2 score) and the EVS are calculated as follows (detailed can be found in [50]):

$$R^2(C_n, \hat{C}_n) = 1 - \frac{\sum_{i=1}^N (C_n^i - \hat{C}_n^i)^2}{\sum_{i=1}^N (C_n^i - \bar{C}_n)^2} \tag{24}$$

$$\text{EVS}(C_n, \hat{C}_n) = 1 - \frac{\text{Var}\{C_n - \hat{C}_n\}}{\text{Var}\{C_n\}} \tag{25}$$

where $\bar{C}_n = \frac{1}{2} \sum_{i=1}^n C_n^i$.

A. Dataset-1: Trimmed Low-Angle-of-Attack Flight Data

2000 data samples (85-s flight duration) of the ATTAS aircraft [8], [9] have been used to train the MFIN with architecture $4 \times (4 \times 3 \times 2) \times 1$ and IPMFs and OPMFs equal to 3 for each node. Network architecture and training information for all other methods are given in Table I.

The parameters of the NN are optimized using gradient descent with momentum, where learning rate $\eta = 0.9$ and the momentum factor $\alpha = 0.1$. The RBFN with the architecture shown in Table I is trained using the recursive least squares (RLS) algorithm [47], [48]; centers of the radial basis function for hidden nodes are obtained from input data using K-means clustering [46]. The T-S FIS [38] is obtained using the training dataset, where premise parts with four fuzzy regions are generated using fuzzy C-means clustering [49], and the consequent parameters are tuned by the RLS algorithm. ANFIS [39], is generated using the MATLAB fuzzy toolbox with the training dataset. The Mamdani FIS [32] with the Gaussian MF in premise and consequent parts is generated using the same training dataset.

The tracking performances of the MFIN and the classical NN for the test dataset and test data corrupted by AWGN with a 40-dB SNR have been shown in Figs. 6–9.

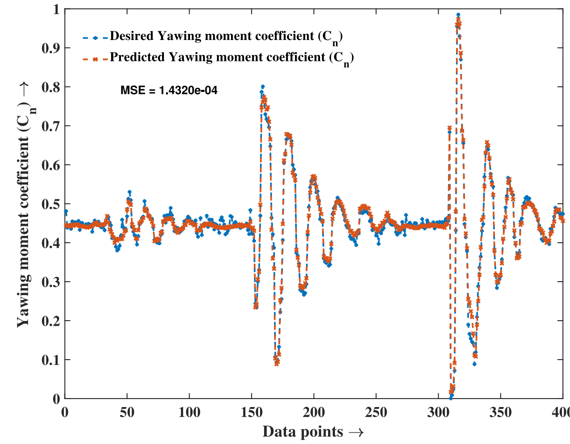

Fig. 6. Performance of MFIN with test dataset-1.

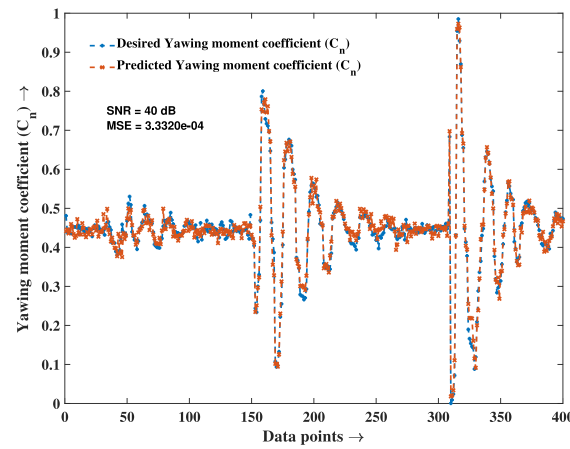

Fig. 7. Performance of the MFIN with test dataset-1 with AWGN.

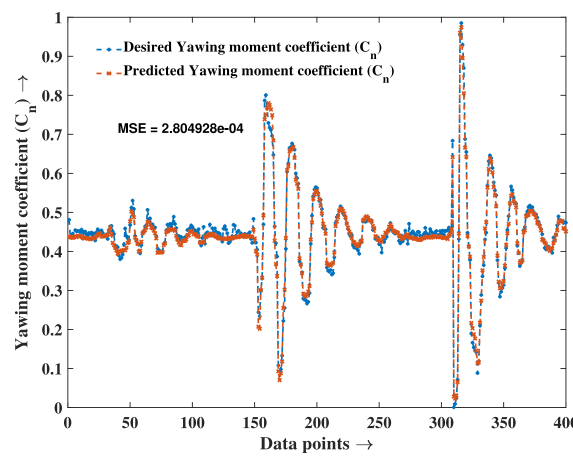

Fig. 8. Performance of the MLNN with test dataset-1.

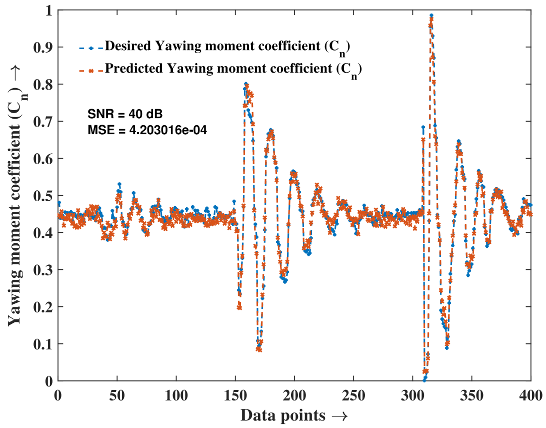

Fig. 9. Performance of the MLNN with test dataset-1 with AWGN.

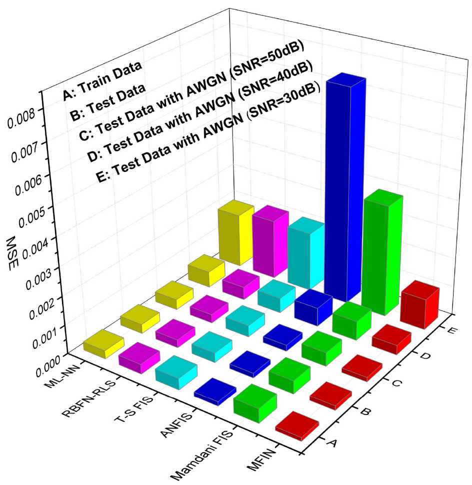

Fig. 10. Comparison of the MSE for the MFIN with state-of-the-art methods.

B. Dataset-2: Quasi-Steady Stall High-Angle-of-Attack (Nonlinear Complex) Flight Data

Nonlinear flight data pairs with 5000 samples (200-s duration, 0.04 samples/s) of the ATTAS aircraft [8], [9] have been used for the identification of the nonlinear aircraft yawing moment coefficient using all above methods with the network architecture of the MFIN as $14 \times (6 \times 3 \times 2) \times 1$ and IPMFs $= 4$ and OPMFs $= 2$ and for all other methods, same as shown in Table I. The tracking performances of the MFIN and the classical NN for the test dataset and test data corrupted by AWGN with the 40-dB SNR have been shown in Figs. 11–14.

To compare the network performance with aforementioned state-of-the-art system identification methods, the MSE, the R^2 score, and the EVS for training data, testing data, and the test data corrupted by AWGN with 50-dB SNR, with 40-dB SNR, and with 30-dB SNR are presented in Tables II and III. It can be observed that the performance of the proposed MFIN is better than the other method even for the test data corrupted with AWGN. The smaller MSE and better R^2 score and explained variance in the case of the MFIN for test data corrupted with AWGN shows the robustness of the proposed method against noise in

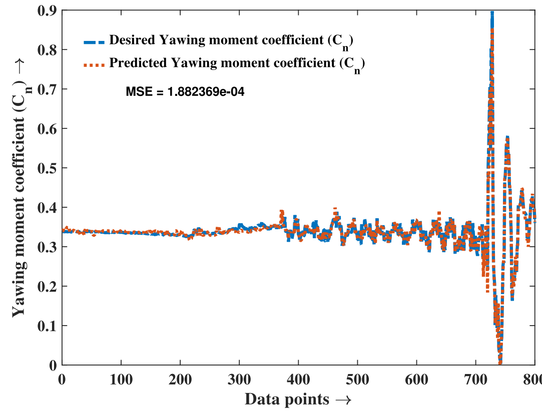

Fig. 11. Performance of the MFIN with test dataset-2.

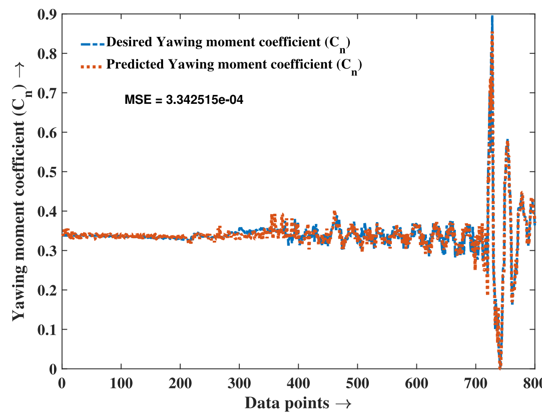

Fig. 12. Performance of MFIN with test dataset-2 with AWGN.

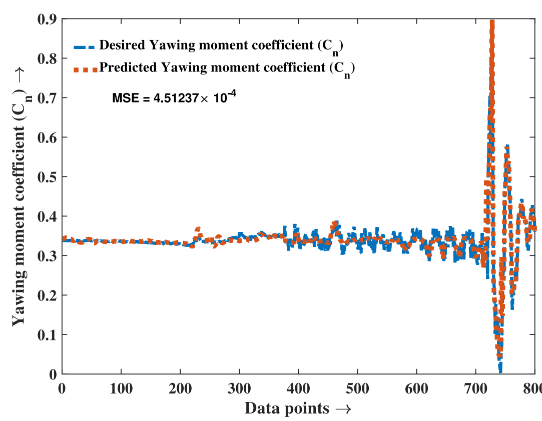

Fig. 13. Performance of MLNN with test dataset-2.

the recorded data. Graphical visualization of variation in the MSE for the first dataset (see Section IV-A) has been depicted in Fig. 10 for better comparison.

C. Time Complexity Analysis

In Table IV, we provide the runtime complexity analysis of the proposed MFIN with comparison to the state-of-the-art methods ML-NN, RBFN-RLS, T-S FIS, ANFIS, and Mamdani FIS in terms of $O(.)$ notation. A detailed study on finding the time complexity of a network can be found in [51]. Let N denote the number of data points, d be the

TABLE II
Comparison of Performance Metrics (MSE, R^2 Score, and EVS) of the MFIN With State-of-the-Art Methods for Dataset-1

Data points/ Methods	Metrics	ML-NN [11]	RBFN-RLS [30]	T-S FIS [38]	ANFIS [39]	Mamdani FIS [32]	**MFIN (Proposed)**
Training Data	MSE	3.90×10^{-4}	9.91×10^{-4}	3.98×10^{-4}	1.80×10^{-4}	4.45×10^{-4}	$\mathbf{1.24 \times 10^{-4}}$
	R^2 Score	0.971	0.974	0.970	0.985	0.967	**0.994**
	EVS	0.973	0.974	0.970	0.985	0.967	**0.994**
Test Data	MSE	2.80×10^{-4}	2.55×10^{-4}	3.08×10^{-4}	1.99×10^{-4}	4.03×10^{-4}	$\mathbf{1.43 \times 10^{-4}}$
	R^2 Score	0.978	0.981	0.976	0.983	0.969	**0.988**
	EVS	0.979	0.981	0.976	0.983	0.971	**0.988**
Test Data with AWGN (SNR = 50 dB)	MSE	3.060×10^{-4}	2.71×10^{-4}	3.29×10^{-4}	2.23×10^{-4}	4.01×10^{-4}	$\mathbf{1.59 \times 10^{-4}}$
	R^2 Score	0.977	0.979	0.975	0.981	0.969	**0.986**
	EVS	0.978	0.979	0.975	0.981	0.971	**0.986**
Test Data with AWGN (SNR = 40 dB)	MSE	4.20×10^{-4}	4.05×10^{-4}	4.91×10^{-4}	1.53×10^{-3}	6.21×10^{-4}	$\mathbf{3.33 \times 10^{-4}}$
	R^2 Score	0.968	0.969	0.962	0.883	0.952	**0.975**
	EVS	0.969	0.969	0.962	0.884	0.955	**0.975**
Test Data with AWGN (SNR = 30 dB)	MSE	1.95×10^{-3}	2.04×10^{-3}	2.13×10^{-3}	3.71×10^{-2}	3.32×10^{-3}	$\mathbf{1.71 \times 10^{-3}}$
	R^2 Score	0.850	0.843	0.836	-1.854	0.744	**0.899**
	EVS	0.851	0.843	0.836	-1.812	0.755	**0.899**

TABLE III
Comparison of Performance Metrics (MSE, R^2 Score, and EVS) of the MFIN With State-of-the-Art Methods for Dataset-2

Data points/ Methods	Metrics	ML-NN [11]	RBFN-RLS [30]	T-S FIS [38]	ANFIS [39]	Mamdani FIS [32]	**MFIN (Proposed)**
Training Data	MSE	2.71×10^{-4}	8.99×10^{-4}	3.03×10^{-4}	2.98×10^{-4}	2.83×10^{-4}	$\mathbf{6.75 \times 10^{-5}}$
	R^2 Score	0.927	0.756	0.918	0.919	0.923	**0.982**
	EVS	0.927	0.756	0.918	0.919	0.923	**0.982**
Test Data	MSE	4.51×10^{-4}	6.72×10^{-4}	4.75×10^{-4}	4.18×10^{-4}	4.59×10^{-4}	$\mathbf{1.88 \times 10^{-4}}$
	R^2 Score	0.869	0.805	0.862	0.879	0.867	**0.945**
	EVS	0.869	0.805	0.862	0.879	0.867	**0.946**
Test Data with AWGN (SNR = 50 dB)	MSE	4.63×10^{-4}	6.76×10^{-4}	4.70×10^{-4}	4.40×10^{-4}	4.44×10^{-4}	$\mathbf{2.26 \times 10^{-4}}$
	R^2 Score	0.866	0.804	0.863	0.872	0.871	**0.934**
	EVS	0.866	0.804	0.863	0.872	0.871	**0.935**
Test Data with AWGN (SNR = 40 dB)	MSE	5.22×10^{-4}	7.03×10^{-4}	6.24×10^{-4}	4.73×10^{-4}	4.36×10^{-4}	$\mathbf{3.34 \times 10^{-4}}$
	R^2 Score	0.848	0.796	0.819	0.863	0.873	**0.903**
	EVS	0.848	0.796	0.819	0.863	0.874	**0.903**
Test Data with AWGN (SNR = 30 dB)	MSE	1.26×10^{-4}	9.51×10^{-4}	1.59×10^{-4}	1.62×10^{-4}	5.50×10^{-4}	$\mathbf{5.50 \times 10^{-3}}$
	R^2 Score	0.635	0.724	0.537	0.528	0.84	**0.84**
	EVS	0.636	0.725	0.537	0.528	0.843	**0.841**

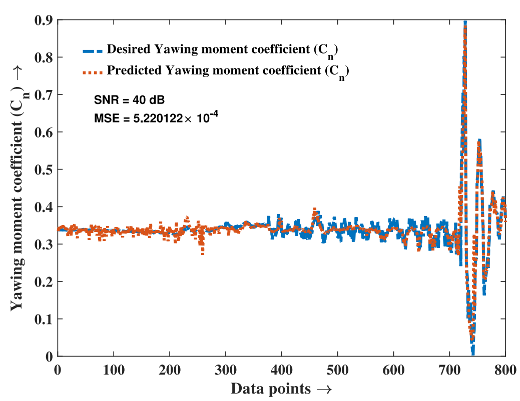

Fig. 14. Performance of the MLNN with test dataset-2 with AWGN.

TABLE IV
Time Complexity of the MFIN and State-of-the-Art Methods

Methodology	Time Complexity
ML-NN [11]	$O(NdLK_l^2)$
RBFN-RLS [30]	$O(N(cd + c^2))$
T-S FIS (with RLS) [38]	$O((\nu^d(d+1))^2)$
ANFIS [39]	$O(N^2\nu^d)$
Mamdani FIS [32]	$O(N\nu^d)$
MFIN (Proposed)	$\mathbf{O(NLK_l^2\nu^d + (LK_l\nu^d)^2)}$

dimensionality of the input data, L be the total number of layers in the network, K_l be the number of nodes in each layer, ν be the number of fuzzy subsets (input fuzzy MF), and c be the number of centers in the RBFN. The maximum number of fuzzy rules for both Mamdani and T-S FISs is given by ν^d, assuming the grid partitioning method of fuzzy rule generation. To obtain time complexity of the MFIN, let us break the operation in two parts: 1) *forward propagation:* assuming neural like operation with ν^d operations per node (Mamdani FIS), time complexity is given by $O(nLK_l^2\nu^d)$; and 2) *parameter optimization using L-BFGS:* time complexity is given by $O(n_p^2)$ [52], where n_p denotes the total number of parameters in the network and is given by $LK_l\nu^d$.

V. CONCLUSION

In this article, we have presented the MFIN with L-BFGS optimization for the identification of nonlinear yawing moment dynamics of the ATTAS aircraft. The neural multilayer network created by using the Mamdani FIS demonstrates its superiority in learning highly nonlinear dynamics, canceling measurement noise from the test data, and handling the data uncertainties. This has been validated on the recorded flight data from the ATTAS aircraft of the DLR German Aerospace Center in two cases: 1) trimmed low-angle-of-attack flight condition and 2) quasi-steady stall high-angle-of-attack (highly nonlinear complex) flight condition. The comparison of the predicted yawing moment coefficients ($\hat{C}_n$) and the true value yawing moment coefficients (C_n) on the both datasets proves that the MFIN can give better prediction even with noisy test data. Also, the comparison of the MSE, the R^2 score, and the EVS shows that the proposed method performs better for the test data as well as the test data corrupted with AWGN; however, the comparable results are observed on the test data without noise for the state-of-art methods.

In [32], it was shown that the Mamdani FIS can easily model the expert opinion and incorporate it as artificial intelligence than the T-S FIS, the ML-NN, and the ANFIS along with the comparable accuracy. Here, it can be observed that the proposed method can have the capability of incorporating expert opinion as well as better accuracy than various state-of-the-art methods of system identification. Also, the trained MFIN is more robust to the noises in the recorded flight data. However, from the time complexity analysis, it can be observed that the proposed method requires high computational resources to train a large number of parameters involved compared to all other state-of-the-art methods. Furthermore, work may be carried out to propose a faster parameter optimization algorithm instead of L-BFGS to reduce the computational time in the training of the MFIN.

ACKNOWLEDGMENT

The authors would like to thank Dr. R. V. Jategaonkar of DLR Germany for providing the permission to use the ATTAS aircraft data.

REFERENCES

[1] Y. Shi, W. Qian, Q. Wang, and K. He
Aerodynamic parameter estimation using genetic algorithms
In *Proc. IEEE Int. Conf. Evol. Comput.*, Vancouver, BC, Canada, 2006, pp. 629–633.

[2] A. Kumar, S. Saderla, and A. K. Ghosh
Aerodynamic parameter estimation using neuro-fuzzy model based method
Proc. 1st Int. Conf. Recent Adv. Aerosp. Eng., Coimbatore, India, 2017, pp. 1–5.

[3] D. Solomatine, L. M. See, and R. J. Abrahart
Data-driven modelling: Concepts, approaches and experiences
In *Practical Hydroinformatics*. Berlin, Germany: Springer, 2009, pp. 17–30.

[4] B. Erol, M. G. Amin, and S. Z. Gurbuz
Automatic data-driven frequency-warped cepstral feature design for micro-Doppler classification
IEEE Trans. Aerosp. Electron. Syst., vol. 54, no. 4, pp. 1724–1738, Aug. 2018.

[5] V. Klein and E. Morelli
Aircraft System Identification: Theory and Practice. Reston, VA, USA: AIAA, 2006.

[6] M. Tischler and R. Remple
Aircraft and Rotorcraft System Identification. Reston, VA, USA: AIAA, 2006.

[7] R. V. Jategaonkar, D. Fischenberg, and W. Gruenhagen
Aerodynamic modeling and system identification from flight data—Recent applications at DLR
J. Aircr., vol. 41, no. 4, pp. 681–691, 2004.

[8] Ravindra V. Jategaonkar
Flight Vehicle System Identification a Time Domain Methodology. Reston, VA, USA: AIAA, 2006.

[9] ATTAS aircraft flight data. [Online]. Available: https://arc.aiaa.org/doi/suppl/10.2514/4.102790, Accessed on: Nov. 5, 2019.

[10] S. E. Lyshevski, K. R. Dunipace, and R. D. Colgren
Identification and reconfigurable control of multivariable aircraft
In *Proc. Amer. Control Conf.*, San Diego, CA, USA, 1999, vol. 4, pp. 2732–2736.

[11] A. K Ghosh, S. C. Raisinghani, and P. K. Kalra
Two new techniques for aircraft parameter estimation using neural networks
Aeronaut. J., vol. 102, no. 1011, pp. 25–29, 1998.

[12] A. K. Ghosh and N. K. Peyada
Aircraft parameter estimation using neural network based algorithm
In *Proc. AIAA Atmos. Flight Mech. Conf.*, Chicago, IL, USA, 2009, pp. 10–13.

[13] S. H. Alsamhi, O. Ma, and M. S. Ansari
Artificial intelligence-based techniques for emerging robotics communication: A survey and future perspectives
2018, *arXiv:1804.09671*.

[14] S. H. Alsamhi, O. Ma, and M. S. Ansari
Predictive estimation of the optimal signal strength from unmanned aerial vehicle over Internet of things using ANN
2018, *arXiv:1805.07614*.

[15] M. S. Seyfioglu, A. M. Ozbayoglu, and S. Z. Gurbuz
Deep convolutional autoencoder for radar-based classification of similar aided and unaided human activities
IEEE Trans. Aerosp. Electron. Syst., vol. 54, no. 4, pp. 1709–1723, Aug. 2018.

[16] B. Jokanovic and M. G. Amin
Fall detection using deep learning in range-Doppler radars
IEEE Trans. Aerosp. Electron. Syst., vol. 54, no. 1, pp. 180–189, Feb. 2018.

[17] D. J. Singh, N. K. Verma, A. K. Ghosh, and A. Malagaudanavar
Fuzzy systems practices for aerodynamic parameter modeling of the aircraft
In *Proc. 6th IEEE Conf. Comput. Appl. Elect. Eng.*, Oct. 5–7, 2017, pp. 462–467.

[18] D. J. Singh, N. K. Verma, A. K. Ghosh, J. Sanwale, and A. Malagaudanavar
Aerodynamic parameter modeling using TS fuzzy systems from flight data
In *Proc. Int. Conf. Comput. Intell.: Theories, Appl. Future Directions*, Dec. 6–8, 2017, pp. 425–437.

[19] M.-Y. Chen and D. A. Linkens
A systematic method for fuzzy modeling from numerical data
Proc. IEEE Int. Conf. Syst., Man, Cybern. e-Syst. e-Man Cybern. Cyberspace, Tucson, AZ, USA, 2001, vol. 1, pp. 28–33.

[20] T. J. Ross
Fuzzy Logic With Engineering Applications, 3rd ed. West Sussex, U.K.: Wiley, 2010.

[21] T. Abdollahi, S. Salehfard, C. H. Xiong, and J. F. Ying
Simplified fuzzy-Padé controller for attitude control of quadrotor helicopters
IET Control Theory Appl., vol. 12, no. 2, pp. 310–317, 2017.

[22] B. Wang, K. Shi, L. Yang, F. Wu, and D. Chen
Fuzzy generalised predictive control for a class of fractional-order non-linear systems
IET Control Theory Appl., vol. 12, no. 1, pp. 87–96, 2017.

[23] F. Li, J. Li, and D. Peng
Identification method of neuro-fuzzy-based Hammerstein model with coloured noise
IET Control Theory Appl., vol. 11, no. 17, pp. 3026–3037, 2017.

[24] X. Tao, J. Yi, X. Tan, and Z. Liu
On the design of fuzzy adaptive state estimator for a flexible air-breathing hypersonic vehicle
Proc. IEEE 14th Int. Conf. Autom. Sci. Eng., Munich, Germany, 2018, pp. 104–109.

[25] Y. Ma and Y. Cai
A fuzzy model predictive control based upon adaptive neural network disturbance observer for a constrained hypersonic vehicle
IEEE Access vol. 6, pp. 5927–5938, 2018.
[26] S. H. Alsamhi, M. Ansari, M. Hebah, A. Ahmed, A. Hatem, and M. Alasali
Adaptive handoff prediction and appreciate decision using ANFIS between terrestrial communication and HAP
SCIREA J. Agriculture. vol. 3, no. 1, pp. 19–33, 2018.
[27] N. K. Verma., V. Singh, S. Rajurkar, and M. Aqib
Fuzzy inference network with Mamdani fuzzy inference system
In *Comput. Intell.: Theories, Appl. Future Directions*, vol. I. Singapore: Springer, 2019, pp. 375–388.
[28] A. K. Sharma, V. Singh, N. K. Verma, and J. Liu
Condition based monitoring of machine using Mamdani fuzzy network
In *Proc. Prognostics Syst. Health Manage. Conf.*, Chongqing, China, 2018, pp. 1159–1163.
[29] S. Saderla, R. Dhayalan, and A. Ghosh
Parameter estimation from near stall flight data using conventional and neural-based methods
Defence Sci. J., vol. 67, no. 1, pp. 03–11, 2011.
[30] J. Sanwale and D. J. Singh
D. J. Aerodynamic parameters estimation using radial basis function neural partial differentiation method
Defence Sci. J., vol. 68, no. 3, pp. 241–250, 2018.
[31] D. J. Singh, P. Agrawal, N. K. Verma, A. K. Ghosh, and A. Malagaudanavar
Interval type-2 TS fuzzy model for angle of attack sensor of the aircraft
J. Intell. Fuzzy Syst., vol. 34, no. 6, pp. 3891–3901, 2018.
[32] A. K. Sharma, D. Singh, and N. K. Verma
Data driven aerodynamic modeling using Mamdani fuzzy inference systems
Proc. Int. Conf. Sens., Diagnostics, Prognostics, Control, Xi'an, China, 2018, pp. 359–364.
[33] B. L. Stevens and F. L. Lewis
Aircraft Control and Simulation. 2nd ed. New York, NY, USA: Wiley, 1992.
[34] J. Roskam
Airplane Flight Dynamics and Automatic Flight Controls. Lawrence, KS, USA: DARcorporation, 1998.
[35] R. W. Beard and W. M. Timothy
Small Unmanned Aircraft: Theory and Practice. Princeton, NJ, USA: Princeton Univ. Press, 2012.
[36] L. X. Wang and J. M. Mendel
Generating fuzzy rules by learning from examples
IEEE Trans. Syst., Man, Cybern., vol. 22, no. 6, pp. 1414–1427, Nov./Dec. 1992.
[37] Nishchal K. Verma and M. Haumandlu
Data driven model using adaptive fuzzy system
Int. J. Autom. Control, vol. 2, no. 4, pp. 447–458, 2008.
[38] T. Takagi and M. Sugeno
Fuzzy identification of systems and its applications to modeling and control
IEEE Trans. Syst. Man, Cybern., vol. SMC-15, no. 1, pp. 116–132, Jan./Feb. 1985.
[39] J.-SR Jang
ANFIS: Adaptive-network-based fuzzy inference system
IEEE Trans. Syst., Man, Cybern., vol. 23, no. 3, pp. 665–685, 1993.
[40] C. G. Broyden
The convergence of a class of double-rank minimization algorithms
J. Inst. Math. Appl., vol. 6, pp. 76–90, 1970.
[41] R. Fletcher
A new approach to variable metric algorithms
Comput. J., vol. 13, pp. 317–322, 1970.
[42] D. Goldfarb
A family of variable metric updates derived by variational means
Math. Comput., vol. 24, pp. 23–26, 1970.
[43] D. F. Shanno
Conditioning of Quasi-Newton methods for function minimization
Math. Comput., vol. 24, pp. 647–656, 1970.
[44] S. Wright and J. Nocedal
Numerical Optimization. New York, NY, USA: Springer, 1999.
[45] R. Fletcher
Practical Methods of Optimization, vols. 1/2. Hoboken, NJ, USA: Wiley, 1980.
[46] J. A. Hartigan and M. A. Wong
Algorithm AS 136: A k-means clustering algorithm
J. Roy. Statist. Soc. Ser. C (Appl. Statist.), vol. 28, no. 1, pp. 100–108, 1979.
[47] L. Behera and I. Kar
Intelligent Systems and Control. Oxford, U.K.: Oxford Univ. Press, Nov. 2009.
[48] Y. Zhang and X. R. Li
Hybrid training of RBF networks with application to nonlinear systems identification
In *Proc. 35th IEEE Conf. Decis. Control*, Kobe, Japan, 1996, vol. 1, pp. 937–942.
[49] J. C. Bezdek, R. Ehrlich, and W. Full
FCM: The fuzzy c-means clustering algorithm
Comput. Geosci., vol. 10, nos. 2/3, pp. 191–203.
[50] S. A. Glantz and B. K. Slinker
Primer of Applied Regression and Analysis of Variance. New York, NY, USA: McGraw-Hill, 1990.
[51] M. Sipper
A serial complexity measure of neural networks
In *Proc. IEEE Int. Conf. Neural Netw.*, San Francisco, CA, USA, 1993, vol. 2, pp. 962–966.
[52] D. R. S. Saputroa and P. Widyaningsih
Limited memory Broyden-Fletcher-Goldfarb-Shanno (L-BFGS) method for the parameter estimation on geographically weighted ordinal logistic regression model (GWOLR)
AIP Conf. Proc., vol. 1868, 2017, Art. no. 040009.

Arun K. Sharma (Student Member, IEEE) received the M.Tech. degree in instrumentation from the Indian Institute of Technology Kharagpur, Kharagpur, India, in 2011. He is currently working toward the Ph.D. degree with the Department of Electrical Engineering, Indian Institute of Technology Kanpur, Kanpur, India.

He is a reviewer for several reputed journals, such as the IEEE TRANSACTIONS ON AEROSPACE AND ELECTRONIC SYSTEMS, the IEEE TRANSACTIONS ON FUZZY SYSTEMS, and the IEEE COMPUTATIONAL INTELLIGENCE MAGAZINE. His research interests include signal processing, machine learning, deep learning, intelligent control systems, intelligent fault diagnosis, fuzzy systems, and their applications.

Dhanjeet Singh (Student Member, IEEE) received the M.S. degree in control and automation in 2018 from the Indian Institute of Technology Kanpur, Kanpur, India, where he is working toward the Ph.D. degree in control and automation.

He is also a Senior Manager (Design) with the Aircraft Upgrade Research and Design Centre, Hindustan Aeronautics Limited, Nasik, India. He has 14 years of experience in flight control and navigation systems of the aircraft. His research interests include artificial intelligence and intelligent control algorithms.

Vikas Singh (Student Member, IEEE) is working toward the Ph.D. degree with the Department of Electrical engineering, Indian Institute of Technology Kanpur, Kanpur, India.

He is a reviewer for several reputed journals, such as the IEEE TRANSACTIONS ON NEURAL NETWORKS AND LEARNING SYSTEMS, the IEEE TRANSACTIONS ON FUZZY SYSTEMS, and the *IEEE Computational Intelligence Magazine*. His research interests include machine learning, deep learning, big data, intelligent data mining, bioinformatics, fuzzy systems, and their applications.

Nishchal K. Verma (Senior Member, IEEE) received the Ph.D. degree in electrical engineering from the Indian Institute of Technology Delhi, New Delhi, India, in 2007.

He is currently a Professor with the Department of Electrical Engineering and Inter-disciplinary Program in Cognitive Science, Indian Institute of Technology Kanpur, Kanpur, India. He has authored or coauthored more than 200 research papers including 55 journals, 167 conferences, four Books (edited/authored), one patent(s) in the field of AI. He has successfully completed 23 projects from various funding agencies such as The BOEING Company, USA, DST, DRDO, JCBCAT, MHRD, SERB, CSIR, IIT Kanpur, MCIT, SFTIG, and VTOL. His research interests include artificial intelligence (AI)-related theories and its practical applications to many interdisciplinary domains but not limited to machine learning, deep learning, computer vision, prognosis and health management, bioinformatics, cyber physical systems/Internet of Things, complex and highly nonlinear systems modeling, clustering, and classifications, etc.

Dr. Verma is an awardee of Devendra Shukla Young Faculty Research Fellowship by the Indian Institute of Technology Kanpur, India, for the year 2013–2016. He has been an Associate Editor/Editorial Board Member of various reputed journals and conferences, which include the IEEE TRANSACTIONS ON NEURAL NETWORKS AND LEARNING SYSTEMS, *IEEE Computational Intelligence Magazine*, and an Editor of IEEE ACCESS. He has also developed several AI-related key technologies for The BOEING Company, USA, and organized AI-related workshops, conferences, seminars, short term courses, etc.